P7.6 COMPARISONS OF DOPPLER VELOCITY TORNADIC VORTEX SIGNATURES WITH SIGNATURES FROM MODEL VORTICES

Rodger A. Brown and Vincent T. Wood
NOAA, National Severe Storms Laboratory, Norman, OK

1. INTRODUCTION

A *tornadic vortex signature* (TVS) exists when a tornado is smaller than the effective half-power beamwidth of the Doppler radar that scans past the tornado; on the other hand, a *tornado signature* exists when a tornado is larger than the beamwidth. The TVS consists of peak flow away from the radar adjacent to peak flow toward the radar. The extreme values are separated azimuthally by about one beamwidth regardless of tornado size or strength based on simulations that assume uniform reflectivity across the tornado (Brown et al. 1978). With the radar beam being wider than the tornado's core diameter, the extreme values of a TVS represent a smeared and degraded version of the tornado. Since Doppler velocity data are collected at discrete azimuthal intervals, the extreme data points do not necessarily represent the absolute extreme values possible.

Investigators who compare Doppler velocity measurements in tornadoes with model vortices typically use the Rankine (1882) Combined Vortex (RCV), which is an artificial blending of two different tangential velocity profiles. With the RCV, tangential velocity increases linearly from the vortex center to a maximum value at the core radius and then decreases as $1/r$ with increasing radius, r (see Fig. 1). However, it has been found that tangential velocities in hurricanes (e.g., Miller 1967) and in tornadoes measured by nearby mobile Doppler radars (e.g., Wurman and Gill 2000; Wurman 2002) decrease beyond the core radius more like $1/r^{0.6}$ with increasing radius. A vortex model employing the $1/r^{0.6}$ factor is called a Modified Rankine Combined Vortex (MRCV; Fig. 1).

Another model that has been applied to tornadoes is the steady-state version of the Burgers (1948)-Rott (1958) Vortex (BRV). The BRV is an exact solution of the Navier-Stokes equations of motion and continuity. The resulting tangential velocity profile represents a balance between inward advection and outward diffusion of angular momentum (Fig. 1).

In this paper, we produce azimuthal profiles of simulated Doppler velocity measurements through the RCV, MRCV, and BRV models. TVS measurements are compared with these simulated TVS profiles to estimate which of the three models best represents the variation of tangential velocities across a tornado.

Corresponding author address: Dr. Rodger A. Brown, National Severe Storms Laboratory, 1313 Halley Circle, Norman, OK 73069; E-mail: Rodger.Brown@noaa.gov

2. METHOD

Simulated TVS profiles are produced by scanning a simulated Doppler radar across analytical one-cell vortex models having uniform reflectivity.

a. Radar simulation

Wood and Brown (1997) describe the analytical model that was used to produce the simulated Doppler velocity data. A three-dimensional radar beam scans past an axisymmetric model vortex and the mean Doppler velocity component of the flow field within the beam is computed. Continuous TVS curves are produced by the model, as compared to data points that are produced at discrete azimuthal intervals by a Doppler radar.

b. Rankine Combined Vortex (RCV)

The RCV is axisymmetric and, for this study, is assumed to be the same at all heights. The tangential velocity (V) distribution across the vortex is specified as

$$V(r) / V_X = (r / r_C)^n , \qquad (1)$$

where V is tangential velocity at radial distance r from the vortex center, V_x is maximum tangential velocity at the core radius r_C, $n = 1$ for $r \le r_C$, and $n = -1$ for $r \ge r_C$. As shown in Fig. 1, the tangential velocity profile has a pointed peak at the core radius (outer edge of core region).

When a Doppler radar scans past a tornado, the magnitude of the TVS is a function of the effective width of the radar beam and the size of the tornado's core region. The effective beam-

width (BW_E) represents a broadening of the beam that is a function of antenna rotation rate, number of pulses transmitted and received, and the time interval between pulses (e.g., Doviak and Zrnić 1993, pp. 193–197). The strength of the TVS decreases as the effective beamwidth becomes increasingly larger than the tornado's core radius (r_C), as illustrated in Fig. 2. With the TVS curves plotted as a function of azimuthal distance divided by BW_E, it becomes evident that the peaks of the curves are separated by an azimuthal distance of approximately one beamwidth.

c. Modified Rankine Combined Vortex (MRCV)

The MRCV is the same as Eq. (1), except that $n = -0.6$ for $r \geq r_C$. The difference between MRCV and RCV is that the tangential velocity for MRCV decreases more slowly with increasing radius beyond r_C (see Fig. 1). TVS curves for the MRCV model, plotted in Fig. 3, are stronger than those for the RCV.

d. Burgers-Rott Vortex (BRV)

The BRV is axisymmetric and can be expressed as

$$V(r)/V_X = 1.398(r_C / r) \{1-\exp[-(1.12\, r / r_C)^2]\} \quad (2)$$

(e.g., Davies-Jones 1983). The tangential velocity profile in Fig. 1 has a rounded peak owing to the balance between inward advection and outward diffusion of angular momentum. The corresponding TVS curves are shown in Fig. 4. The BRV TVSs likewise are stronger than the RCV TVSs. However, relative to the MRCV curves, the less degraded BRV TVSs (that is, smaller BW_E/r_C ratios) are stronger than the MRCV TVSs, while the more degraded BRV TVSs are weaker.

e. TVS curves plotted as a function of normalized azimuthal distance

The curves in Figs. 2–4 can be used to construct sets of TVS curves that have the same peak velocities. An example of TVS curves having the same peak value of 40 m s^{-1} for three BW_E/r_C ratios for the RCV model is plotted in Fig. 5 as a function of normalized azimuthal distance (azimuthal distance divided by effective beamwidth). Referring to Fig. 2, one may note that the peaks of the $BW_E/r_C = 3$ curve have normalized values of ±0.53. In order for the peaks to be ±40 m s^{-1} (= ±0.53 V_X), the maximum tangential velocity would have to be 76 m s^{-1}. For the peaks of the $BW_E/r_C = 5$ curve (±0.38) to be ±40 m s^{-1} (= ±0.38 V_X), the maximum tangential velocity would have to be 106 m s^{-1}. Similarly, for the peaks of the $BW_E/r_C = 10$ curve (±0.21) to be ±40 m s^{-1}, the maximum tangential velocity would be an unrealistically large value of 192 m s^{-1}.

The fact that the three curves in Fig. 5 are nearly identical indicates that one cannot estimate the size or strength of a tornado from its Doppler velocity signature when the tornado is smaller than the radar's beamwidth. Curves similar to those in Fig. 5 were computed for each of the three vortex models for TVS peak values between 15 and 55 m s^{-1} at 5 m s^{-1} intervals.

A comparison of the 40 m s^{-1} curves for the RCV and MRCV models is shown in Fig. 6. Since the tangential velocities outside the core region are stronger for the MRCV model (Fig. 1), it is not surprising that the corresponding 40 m s^{-1} curves have stronger Doppler velocity values. However, looking at the RCV and BRV curves in Fig. 7, it *is* surprising that the two sets of curves are essentially identical. A BRV tornado whose core radius is 1/3 the effective beamwidth and peak tangential velocity is 59 m s^{-1} has basically the same Doppler velocity measurements as a RCV tornado whose core radius is 1/10 the beamwidth and peak rotational velocity is 192 m s^{-1}. Since the BRV and RCV Doppler velocity curves are so similar, only the BRV curves will be used for the data comparisons.

3. DATA COMPARISONS WITH ANALYTICAL VORTEX MODELS

The procedure was to determine which vortex model best fitted Doppler velocity measurements made across tornadoes. Two data sets were selected for the comparisons: the TVSs associated with the Union City, OK tornado of 24 May 1973 (Brown et al. 1978) and the TVSs associated with the first of a series of tornadoes on 16 May 1995 that started near Garden City, KS and moved to the east-northeast (e.g., Brown 1998; Wakimoto and Liu 1998). TVS-like shear regions (data points at 1.0° azimuthal intervals) were measured at 26 elevation angles during the duration of the Union City tornado (37–67 km from the NSSL Norman Doppler radar that had an effective beamwidth of 0.9°) and 33 during the duration of the Garden City tornado (71–87 km from the Dodge City WSR-88D radar that has an effective beamwidth of 1.29°).

The process for fitting these data points to the most appropriate curve follows Brown (1998). Briefly, Doppler velocity data points for a particular

TVS were plotted on a blank version of Fig. 5 (that is, one without the curves). One of the extreme data points was plotted at zero distance and the others were plotted relative to it at azimuthal increments divided by the effective beamwidth of the radar. A series of different TVS curves were then laid over the data point plot and shifted up and down and left and right trying to obtain the best fit for one set of curves. In order to have a fit, a minimum of three data points straddling the center of the TVS had to fall on a set of model curves.

Twenty-three of the 26 Union City shear regions and 22 of the 33 Garden City shear regions satisfied the fit requirement. Those TVS-like shear regions that did not fit the curves occurred at the beginning or end of the tornado's life cycle. For about one-quarter of the shear regions that did fit the curves, the same number of data points fit both the BRV/RCV and MRCV curves; for about half of these a stronger BRV/RCV Doppler velocity curve was needed to pass through the data (Fig. 8). Of the remaining cases, not all the data points fit one, the other, or both of the curves. Examples of two such cases are shown in Figs. 9 and 10, respectively.

Overall characteristics of the fit of Doppler velocity data points to the MRCV and BRV/RCV model curves are summarized in Figs. 11–13. Of the data points measured through the two tornadoes, four to five adjacent data points typically coincided with one of the simulated TVS curves (Fig. 11).

The frequency distribution in Fig. 12 shows the differences in the number of data points that fit the MRCV and BRV/RCV curves. For the vast majority, the number of data points is the same or differs by only one, and there is no preference toward one model curve or the other.

In about half the cases, MRCV and BRV/RCV curves having the same peak Doppler velocity values fit a given set of data points (center bar in Fig. 13). However, when curves having different peak Doppler velocity values provide the best fit, the BRV/RCV curve nearly always has the stronger peak velocity value (as shown in Fig. 8).

4. DISCUSSION

In this study, we compared Doppler radar data collected through two tornadoes with simulated TVS profiles based on three different vortex models. A uniform distribution of reflectivity across the tornado was assumed. We found that the Rankine Combined Vortex and Burgers-Rott Vortex produced essentially identical TVS profiles. The TVS profile for the Modified Rankine Combined Vortex had stronger Doppler velocity values outside the core region than did the profiles for the other two model vortices.

Overall, the four to five data points closest to the center of the tornado fit the BRV/RCV and MRCV TVS profiles equally well. Since the tails of the BRV/RCV profile were weaker than those of the MRCV profile, a BRV/RCV profile with a stronger velocity peak frequently was required to fit the data points. Therefore, it appears that, at least for data collected at 1.0^{o} azimuthal intervals, TVS curves based on the RCV, MRCV, and BRV models all do an equally credible job in fitting the measurements.

Proximity ground-based and airborne Doppler radar measurements in tornadoes reveal the presence of a weak reflectivity core region (e.g., Wakimoto and Martner 1992; Wakimoto et al. 1996; Wurman and Gill 2000). One might argue that the uniform distribution of reflectivity that we used across our model tornadoes is unrealistic. However, we have started to use high-resolution numerical simulations of tornadoes to produce weak reflectivity core regions (caused by centri-fuging of radar scatterers) and associated radial, tangential, and vertical velocity fields that we can scan with our simulated radar. Preliminary analyses indicate that, beyond about 40 km, there is so much smearing by the broad radar beam that there is little difference in TVS curves between tornadoes with weak reflectivity cores and those with uniform reflectivity. Therefore, based on the good fit of the measurements to the theoretical TVS curves and the fact that the tornadoes in this study were about 40–90 km from the radars, the use of uniform reflectivity across the model tornadoes appears to be justified for the comparisons made in this study.

5. REFERENCES

Brown, R. A., 1998: Nomogram for aiding the interpretation of tornadic vortex signatures measured by Doppler radar. *Wea. Forecasting*, **13**, 505–512.

_____, L. R. Lemon, and D. W. Burgess, 1978: Tornado detection by pulsed Doppler radar. *Mon. Wea. Rev*., **106**, 29–38.

Burgers, J. M., 1948: A mathematical model illustrating the theory of turbulence. *Adv. Appl. Mech*., **1**, 197–199.

Davies-Jones, R. P., 1983: Tornado dynamics. *Thunderstorm morphology and dynamics*, E.

Kessler, Ed., Univ. of Oklahoma Press, 197–236.

Doviak, R. J., and D. S. Zrnić, 1993: *Doppler Radar and Weather Observations*. 2nd ed., Academic Press, 562 pp.

Miller, B. I., 1967: Characteristics of hurricanes. *Science*, **157**, 1389–1399.

Rankine, W. J. M., 1882: *A Manual of Applied Physics.* 10th ed., Charles Griffin and Company, London, 663 pp.

Rott, N., 1958: On the viscous core of a line vortex. *Z. Angew. Math. Physik*, **96**, 543–553.

Wakimoto, R. M., and B. E. Martner, 1992: Observations of a Colorado tornado. Part II: Combined photogrammetric and Doppler radar analysis. *Mon. Wea. Rev.*, **120**, 522–543.

_____, and C. Liu, 1998: The Garden City, Kansas, storm during VORTEX 95. Part II: The wall cloud and tornado. *Mon. Wea. Rev.*, **126**, 393–408.

_____, W.-C. Lee, H. B. Bluestein, C.-H. Liu, and P. H. Hildebrand, 1996: ELDORA observations during VORTEX 95. *Bull. Amer. Meteor. Soc.*, **77**, 1465–1481.

Wood, V. T., and R. A. Brown, 1997: Effects of radar sampling on single-Doppler velocity signatures of mesocyclones and tornadoes. *Wea. Forecasting*, **12**, 928–938.

Wurman, J., 2002: The multiple-vortex structure of a tornado. *Wea. Forecasting*, **17**, 473–505.

_____, and S. Gill, 2000: Finescale radar observations of the Dimmitt, Texas (2 June 1995), tornado. *Mon. Wea. Rev.*, **128**, 2135–2164.

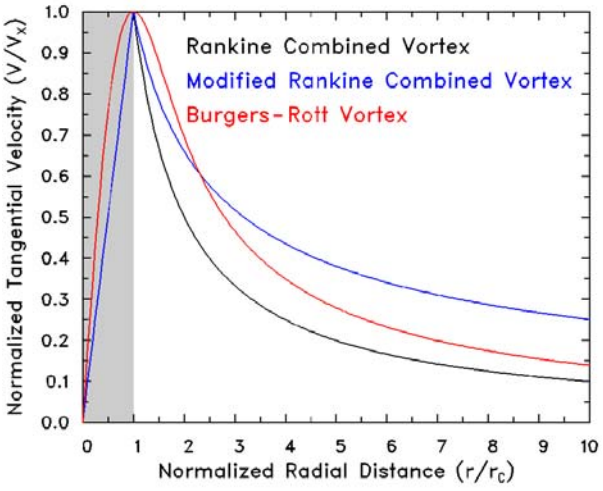

Fig. 1. Normalized tangential velocity distributions for three vortex models. Shaded area is the core region.

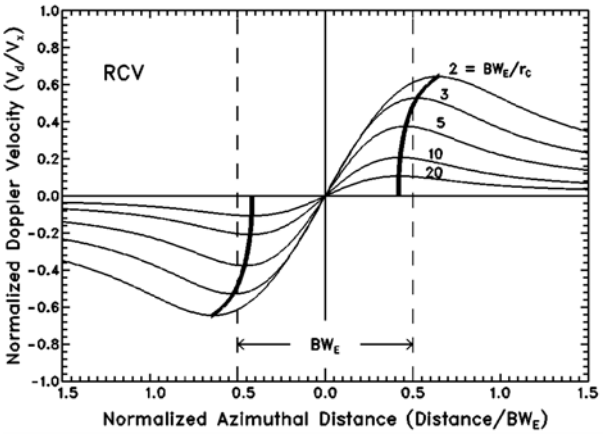

Fig. 2. Doppler velocity tornadic vortex signature curves through the center of a Rankine Combined Vortex for various ratios of effective beamwidth (BW_E) to vortex core radius (r_C).

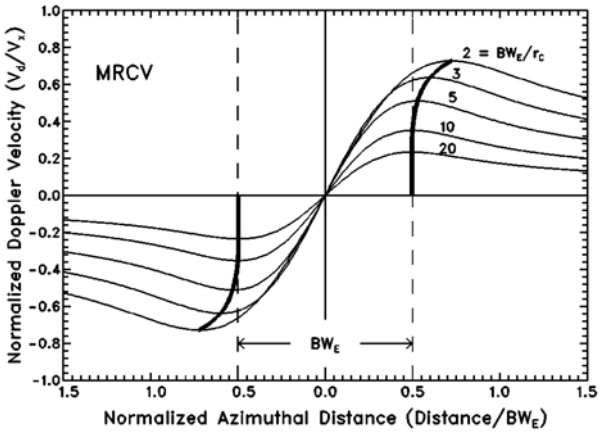

Fig. 3. Same as Fig. 2 except for Modified Rankine Combined Vortex.

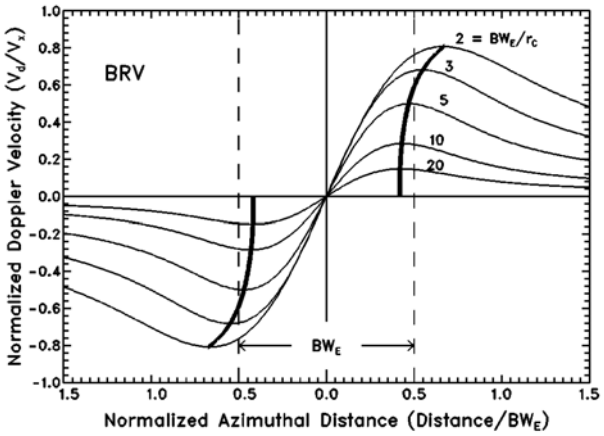

Fig. 4. Same as Fig. 2 except for Burger-Rott Vortex.

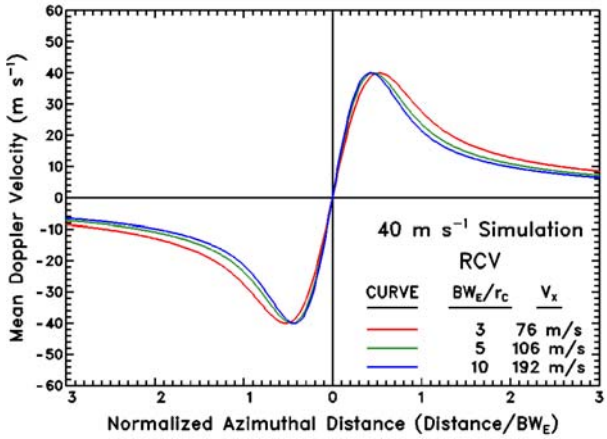

Fig. 5. Three TVS curves from Fig. 2 set equal to peak values of ±40 m s^{-1}.

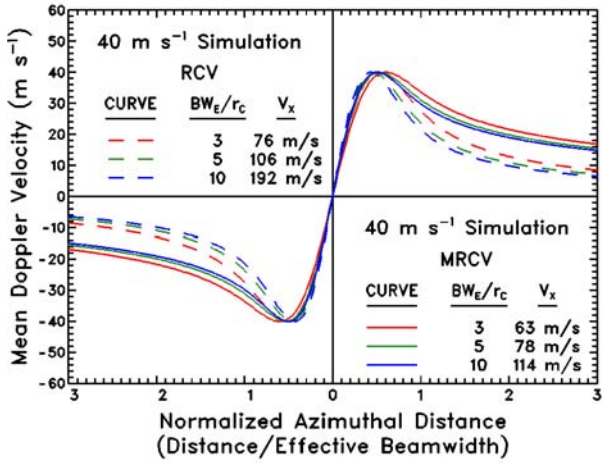

Fig. 6. Comparison of TVS curves for RCV and MRCV set equal to peak values of ±40 m s^{-1}.

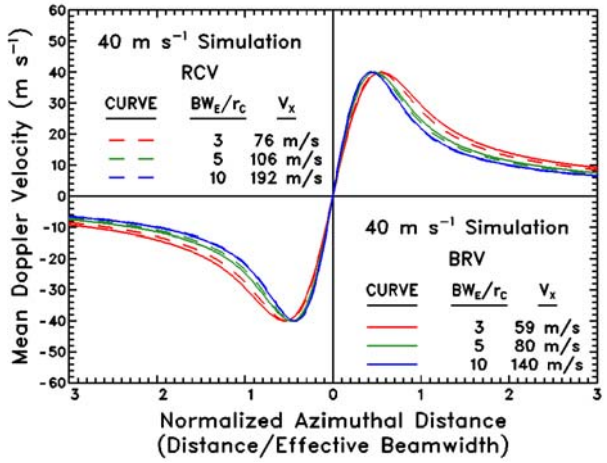

Fig. 7. Comparison of TVS curves for RCV and BRV set equal to peak values of ±40 m s^{-1}.

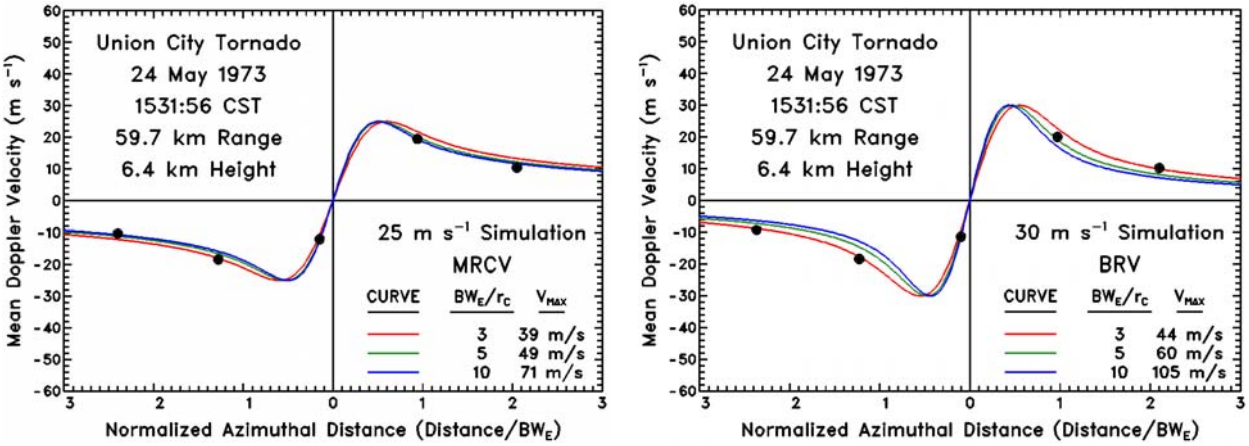

Fig. 8. Fitting of Doppler velocity measurements from the Union City tornado to simulated TVS profiles derived from (left) MRCV and (right) BRV/RCV models.

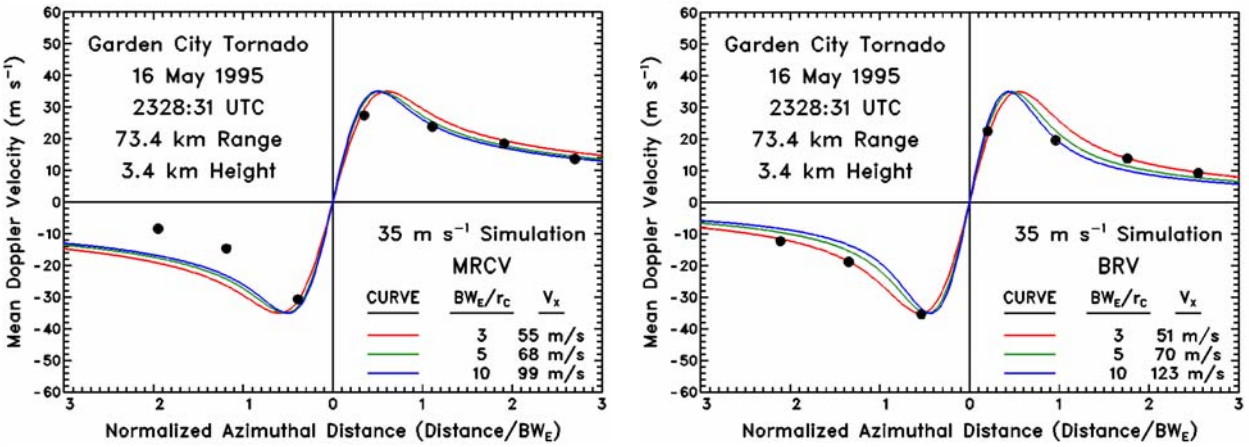

Fig. 9. Same as Fig. 8, except for Garden City tornado at 2328:31 UTC.

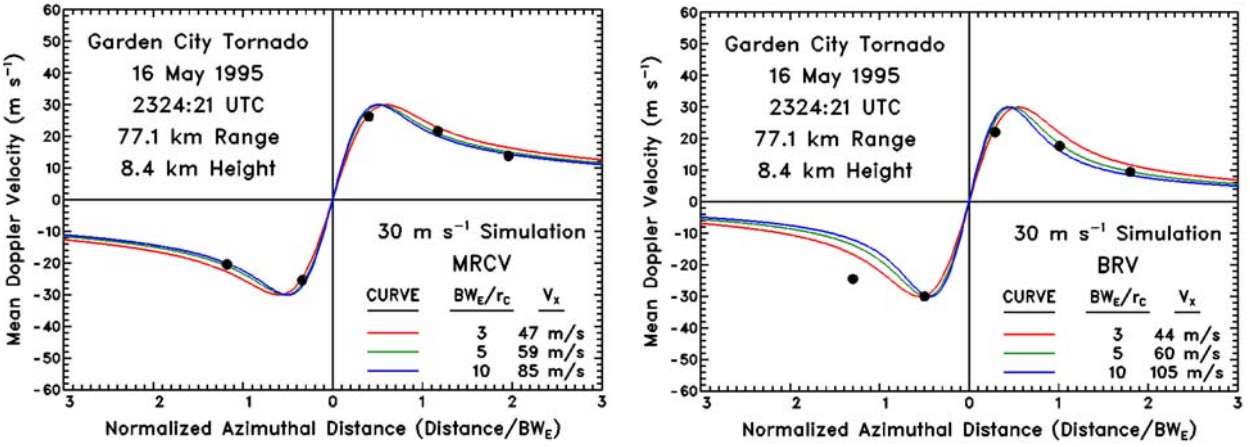

Fig. 10. Same as Fig. 8, except for Garden City tornado at 2324:21 UTC.

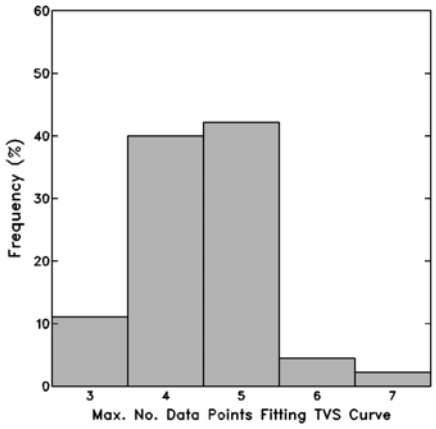

Fig. 11. Frequency distribution of the maximum number of data points fitting one or both of the simulated TVS curves for each MRCV–BRV/RCV pair.

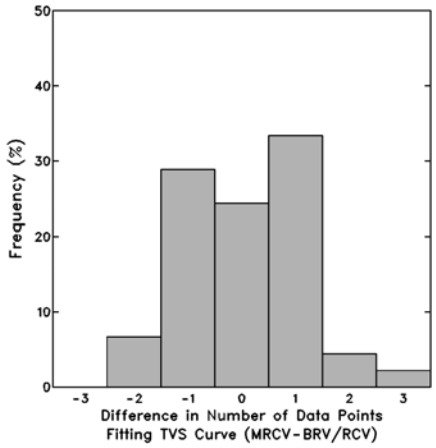

Fig. 12. Frequency distribution of the difference in the number of data points fitting the simulated TVS curves for each MRCV–BRV/RCV pair.

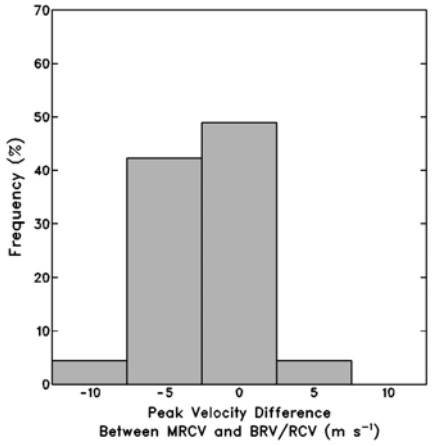

Fig. 13. Frequency distribution of the difference in the peak value of the best-fit simulated TVS curves for each MRCV–BRV/RCV pair.